GECO-DOSY Post-Processing Analysis of Polymers

Kristofer J. Thurecht, Steven M. Howdle, Adrienne L. Davis, and Jason R. Hyde*

School of Chemistry, University of Nottingham, Nottingham NG7 2RD, UK

Received June 16, 2006; Revised Manuscript Received December 5, 2006

ABSTRACT: Generalized correlation diffusion ordered spectroscopy (GECO-DOSY) has been employed to increase the resolution of a more traditional DOSY experiment. We have compared purely linear polycaprolactone (PCL) with that of a sample that also contains impurities, probably small cyclic oligomers formed as a side product in the polymerization experiment. In low concentrations, cyclic PCL with more than two monomer units is not normally detectable by ^{1}H NMR, as there is little chemical shift contrast between the macrocyclic and linear environments. However, analysis with GECO-DOSY allowed mathematical deconvolution of the NMR spectrum and revealed that additional signals were present that were masked by the more intense linear PCL. This is the first use of GECO-DOSY for analysis of polymer experimental data and has proved that the technique has useful applications for polymer characterization. We also examine the effects of instrument errors commonly associated with DOSY in conjunction with the use of GECO-DOSY.

Introduction

Enzymatic-mediated polymerizations have received increasing popularity over the previous half a decade due to the concept of replacing potentially toxic and damaging metal catalysts with a "greener" alternative.[1−5] One polymerization process that has found particular popularity is the enzymatic ring-opening polymerization (eROP) of ϵ-caprolactone to yield the linear polymer. *Candida Antarctica* lipase B (CALB) is particularly effective for this polymerization, giving high yields of a relatively high molecular weight polymer with a polydispersity typically less than 2.[6−8] In a recent publication, we showed that CALB immobilized on a crosslinked resin (Novozym-435) was an effective catalyst for the polymerization of caprolactone in supercritical CO_2.[9] While effective conversion of monomer is readily achieved in the presence of catalyst, considerable side-reactions have been shown to occur and, indeed, predominate at high monomer conversions.[10] One important reaction is the enzyme-catalyzed formation of cyclic polymer *via intra*molecular trans-esterification.[11] Quick and easy quantification of the cyclic component in an eROP process has proven difficult due to the relatively small amount of cyclic component in the polymer and also the inability to differentiate between cyclic and linear polymer using conventional characterization methods (i.e. ^{1}H NMR).

Diffusion ordered spectroscopy (DOSY) is one of the many powerful experimental techniques available to the NMR spectroscopist.[12−19] Available on almost any modern commercial NMR spectrometer, the DOSY experiment provides a convenient method of separating analytical signals from species that exhibit different diffusion coefficients and hence molecular weight in the case of polymers[18,20,21] instead of those with a specific spin system.[13] The DOSY experiment is often applied to a mixture of molecules of known composition.[22] However, increasingly, it has also been applied to mixtures of unknown composition and serves as an analytical method for aiding structure determination. An ideal DOSY analysis would provide precise and accurate diffusional information while providing resolution in the chemical shift domain; this goal is, however, often difficult to achieve. The causes of experimental problems often arise from the NMR probe design, and so pulse sequences need to be chosen accordingly. There are several excellent reviews that cover in depth the details of the experimental methods[14,19,23] and postprocessing methods (DECRA, SVD, MCR etc.),[24−26] which aim to maximize either resolution in the chemical shift domain or in the diffusion domain. Indeed, recent advances in probe and pulse sequence design, along with the advent of more powerful field gradients (allowing the study of more slowly diffusing species), has led to the increased application of DOSY to polymer mixture characterization.[18,20,21,27−29] In general, the DOSY experiment is easy to perform and, providing there is suitable chemical shift and diffusion contrast, good analysis of individual components can be performed. Limitations of the method exist when the diffusion coefficients of individual species are similar, if the NMR signals overlap, or if the polymer has high molecular weight dispersity. In this paper, we describe the use of the generalized correlation function (GCF) as a practical method for overcoming the limitations of the traditional DOSY experiment. In particular, we show that the GCF can be useful for identification of analytical signals that arise from species with very similar self-diffusion coefficients or chemical shifts.[30] Furthermore, we show that this analytical method is particularly suited to the characterization of products resulting from the eROP of caprolactone because the cyclic and linear polymer exhibit very similar chemical shifts and diffuse at similar rates when the cyclic component of the mixture is in a low concentration.

Theoretical Basis

The GCF has been widely applied to vibrational spectroscopic methods[30] such as infrared, Raman, and NIR spectroscopy;[31−37] more recently its use has been widened to chromatographic techniques.[38−40] Eades and Noda have already shown that the GCF can be applied to DOSY (GECO-DOSY), providing good resolution in both the diffusion and chemical shift domains.[30] Their examples showed that closely overlapped signals could be differentiated and that the data could be presented in a more traditional contour plot of chemical shift versus diffusion coefficient. Noda and Ozaki also provided proof that each pair of correlated signals was proportional to the natural logarithm of the ratio of diffusion coefficients for exponentially decaying dynamic signals, thus providing quantitative information pro-

* Corresponding author. E-mail: jason.hyde@nottingham.ac.uk.

10.1021/ma061345q CCC: $37.00
Published on Web 01/27/2007

vided a known diffusion coefficient is present in the analysis.[41] A brief outline of the GCF as applied to decaying signals is given below in order to demonstrate the ease with which the GECO-DOSY approach can be applied to traditionally collected data.[41]

The GCF takes the general form, shown in eq 1, and relates the degree of correlation between two independent signals at coordinates δ_1 and δ_2 while undergoing a perturbation. In the case of a DOSY experiment, the perturbation applied, *G*, is the gradient strength (*G* represents the perturbation of the field gradient strength, while *g* represents the gradient strength in a particular experiment). ν represents the Fourier frequency[45] of the signal with respect to the gradient strength, *g*, and $\tilde{Y}_1(\upsilon)$ is the Fourier transform of the variation in the intensity of the chemical shift, δ_1. $\tilde{Y}_2^*(\upsilon)$ is the forward conjugate of the Fourier transform of the variation in the intensity of the resonance with respect to *g*, at a chemical shift of δ_2.

$$\Phi(\delta_1,\delta_2) + i\Psi(\delta_1,\delta_2) = \frac{1}{\pi\,(G_{\max} - G_{\min})} \int_0^\infty \tilde{Y}_1(\upsilon)\cdot \tilde{Y}_2^*(\upsilon)\,\mathrm{d}\upsilon \quad (1)$$

The form of the GCF splits the signal into real and imaginary components. The real component, Φ, represents the synchronous relationship and describes the degree of similarity of two signals at independent chemical shifts: because in the case of DOSY measurements, all signals decay during the perturbation, *g*, this part of the solution is discarded. The imaginary component, Ψ, describes the "out-of-phase" relationships between two independent chemical shifts. These vary at different rates depending on the diffusion coefficients. In this case, signals that arise from the same molecular species diffuse at the same rate and there is complete synchronicity between them; hence Ψ is equal to zero. If, however, the correlation between two δs arises from species that diffuse at different rates, Ψ will be nonzero: it is these cross-correlations that provide the resolution between species.

Practically, the calculation is simple to apply to data recorded from a DOSY experiment, provided that the perturbation (Δg) between each experiment is well-defined and kept constant. A detailed description of calculating the asynchronous analysis is not provided here as it has been described elsewhere.[30,36,37,42]

In this paper, we have concentrated on the asynchronous signals obtained from the OCH_2 resonance on the PCL backbone in order to reveal if the macrocyclic signals can be distinguished from the larger linear component. In this sense, the analysis is limited to the correlations associated with these triplet resonances, centered at 4.004 ppm, although the technique can be applied to the whole chemical shift range if required.

Experimental

A sample of purely linear polycaprolactone (PCL-1) was obtained from Sigma Aldrich and used as received. The molecular weight of the polymer fraction was 10 kDa with a very narrow polydispersity (1.04). A second sample of PCL (PCL-2) was synthesized by enzyme-catalyzed ring-opening polymerization in supercritical CO_2 as published previously. Typically, 0.4 g of Novozym-435 (10 wt % *Candida antarctic* lipase B immobilized on an acrylic resin) was dried under vacuum (<10 mTorr) for 16 h at 35 °C in a high-pressure autoclave. ϵ-Caprolactone monomer (5 mL, predried over calcium hydride, followed by distillation under vacuum) was added to the autoclave under a positive flow of CO_2 to prevent the ingress of moisture into the system. The autoclave was sealed, pressurized to 1500 psi, and stirred by way of a magnetic stirrer bar in the autoclave. The reaction was allowed to proceed for 24 h, during which time 100% conversion of monomer was attained.

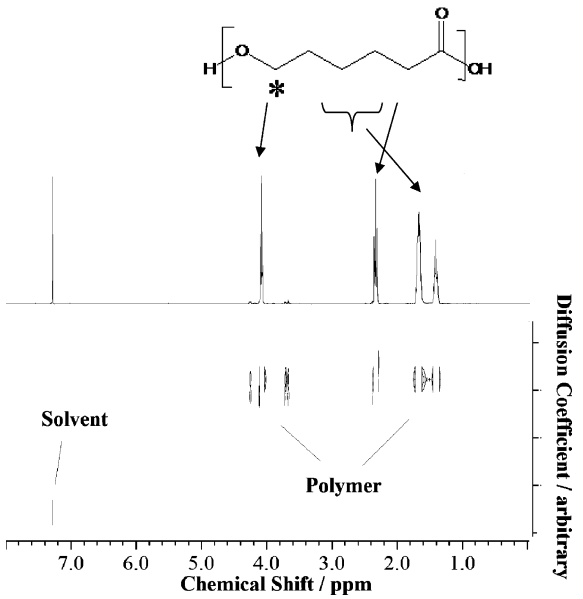

Figure 1. Conventional DOSY spectrum of PCL formed by enzymatic polymerization (PCL-2). The figure clearly shows the poor contrast in diffusion coefficients in the polymer region of the spectrum with only a single diffusion species being observed. The protons that give rise to the triplet used in this report are marked with a star. The rapidly diffusing $CDCl_3$ solvent peak is labeled.

Upon depressurization, the product was dissolved in chloroform, filtered to remove the enzyme, and precipitated in cold methanol. The resulting polymer had M_n of approximately 15 kDa and a polydispersity of 1.8.

DOSY experiments were performed on a Bruker AV400 spectrometer (400.13 MHz for ^{1}H) using a BBO probe with *z*-gradients. The polymer was dissolved in $CDCl_3$ for analysis. To reduce the effects of convection during the diffusion experiment, the data was acquired at 25 °C with a nitrogen flow rate of 535 L h^{-1}. Furthermore, the pulse sequence of Jerschow and Muller,[43] consisting of a double stimulated echo with bipolar gradient pulses modified to reduce the constant velocity effects of convection, was utilized. The gradient pulse time was set to 8 ms with a diffusion time of 140 ms. The maximum gradient strength of the probe was 53 G cm^{-1}, and this was increased linearly over 24 experiments from 2 to 95% gradient strength. Typically, 32 scans were co-added to increase signal-to-noise for each experiment.

DOSY data were exported into Matlab (Mathworks, Inc. R14) from a comma-separated value (CSV) export from MestreC. The asynchronous calculation was performed by scripts written in-house (Supporting Information). The signal used for analysis in this report was the OCH_2 triplet of PCL, centered at 4.004 ppm.

Results and Discussion

Polymer Analysis by Conventional DOSY and GECO-DOSY. The formation of cyclic PCL oligomers during eROP of caprolactone has been well documented in the literature.[11] Indeed, such species are predicted by the accepted mechanism of CALB-catalyzed polymerization and is believed to be related to the concentration of initiator present during polymerization. Figure 1 shows the ^{1}H NMR spectrum of PCL-2 along with the conventional DOSY spectrum of the data. The spectrum consists of both linear and cyclic PCL, however, conventional DOSY analysis is clearly unable to distinguish between the two species. This is due to the fact that there is little chemical shift dispersion between cyclic oligomers with more than three monomer units and linear PCL. Hence, the DOSY experiment shows a broad dispersion of diffusion coefficients for PCL (as might be expected for a polydisperse polymer). Indeed, the DOSY map of PCL-1 and PCL-2 are identical. This highlights

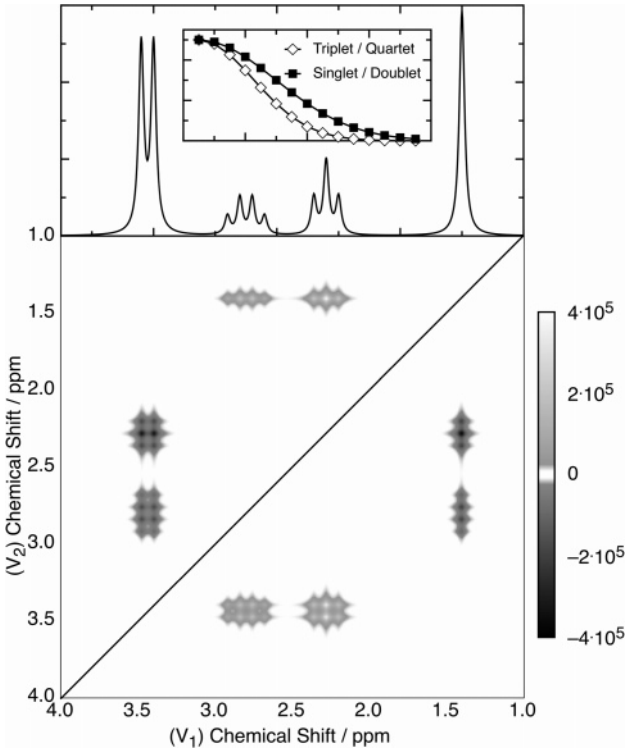

Figure 2. Asynchronous correlation plot produced by the Gaussian decay of a simulated NMR spectra for resonances of two independent species. The off-diagonal cross-correlations [at coordinates ψ(3.5 ppm, 2.75 ppm) and ψ(3.5 ppm, 2.25 ppm)] show that the two resonances decay at different rates.

the problems associated with conventional DOSY analysis for polymers having components that are very similar in nature.

To extract meaningful information from the DOSY data, generalized correlation (GECO) analysis was performed on the DOSY spectra of PCL-1 and PCL-2. The results are presented in the following sections and a direct comparison is made between the two data sets.

Ideal Gaussian Decay. To demonstrate GECO-DOSY and understand instrumental effects and how they manifest themselves, an ideal signal, a broadening resonance, and frequency shifting resonances have been simulated. We apply this approach to the characterization of purely linear polycaprolactone and a linear/cyclic mixture synthesized via enzymatic ring-opening polymerization.

Figure 2 shows the asynchronous correlation plot of a simulated NMR spectrum consisting of two Gaussian decaying species. The spectrum contains a singlet, doublet, triplet, and quartet to demonstrate the correlation maps obtained during the GECO-DOSY analysis: the singlet and doublet are resonances from the same species, the triplet and quartet are similarly related, the Gaussian decay intensities for each species are indicated in the inset of the spectra. As can be seen, there are two off-diagonal correlation signals between each of the species (positive correlations are represented by gray/white and negative by gray/black). These cross-correlations indicate that the signals decay with differences in *D*; in fact, by applying Noda's rules, it is possible to ascertain that the resonances of the quartet and triplet decay faster than the resonances from the singlet and doublet (i.e., they have a larger value of *D*). The absence of cross-correlations between the doublet and singlet, ψ(3.5 ppm, 1.5 ppm), indicate that the resonances arise from the same species; the same is true of the quartet and triplet. Because all DOSY signals decay with a positive synchronous relationship, the application of Noda's rules becomes particularly simple: coupling between resonances that produce positive cross-correlations diffuse at a faster rate than couplings that have negative cross-correlations, i.e., in this example, the cross-correlation at ψ(2.75 ppm, 3.5 ppm) indicates that the first coordinate signal (2.75 ppm) is the faster decaying resonance. This conclusion can be confirmed by examining the Gaussian decay intensities, which clearly show that the quartet/triplet peaks decay faster (larger *D* coefficient) than the singlet/doublet resonances.

In the above example, the four sets of resonances have clear chemical shift resolution; however, cross-correlations that arise close to the $\psi(\nu_1,\nu_1)$ diagonal indicate the presence of two species with little chemical shift contrast. Noda et al. have previously shown this resolution, where a clear δ resolution between two different species in the GECO-DOSY maps is present, even though the NMR resonances were close. The excellent chemical shift discrimination of this technique also does not infringe on the *D*-domain resolution: under ideal conditions (low noise and high numerical accuracy), the *D*-domain resolution is large and two resonances can still be differentiated at a δ resolution of 1 data point. This exceptional resolving power promotes GECO-DOSY as an extremely powerful technique for DOSY analysis and is of a particular utility to polymer mixtures where compounds may have very similar self-diffusion coefficients.

Line Narrowing/Broadening. Line broadening is a common artifact of a DOSY experiment and is caused by a time-dependent inhomogeneity in the magnetic field.[44] This loss of homogeneity broadens the signal received by the spectrometer. The rate of line broadening is proportional to the rate of loss of homogeneity; this may introduce a fortunate advantage for GECO-DOSY as line-broadening will appear in the asynchronous cross-correlations between different species, which due to differences in molecular weight exhibit different natural broadening coefficients. GECO-DOSY analysis treats this data in a unique manner that is easily identified as a horizontal/vertical cross-shape in each correlation map that is centered about the resonance maximum. This pattern has previously been identified and simulated as a line-broadening feature in FTIR data. Figure 3 presents two Lorentzian resonances that have been broadened at a small but constant rate, while the signal intensity decays in a Gaussian fashion.

As evident in Figure 3, the cross-correlations between each signal present themselves as the cross-shape, with the positive nodes (gray/white) projecting horizontally and the negative nodes (gray/black) pointing vertically. This behavior can be explained by the broadening of the resonance; as the overall signal intensity decays, the relative contribution toward the base of the resonance increases and thus is positively correlated to the peak maxima, which does not exhibit any broadening. The positive/negative nodes would be reversed if the resonances were to be sharpening during the exponential decay. The greater the degree of line broadening, the greater in size each of the lobes associated with the resonance. It should be noted that this effect produces much weaker correlation signals than if there were two species present (compare legend scales). Thus, it is possible to detect any line broadening that is occurring during the acquisition of the DOSY experiment. The fact that the overall signal intensity is decaying does not affect this correlation as it can with peak shifting.

Peak Shifting. A variation of resonance frequency is one of the most difficult correlations to interpret when in conjunction with decaying resonance intensity. If the resonance intensity were not decaying, the phenomenon would easily be distin-

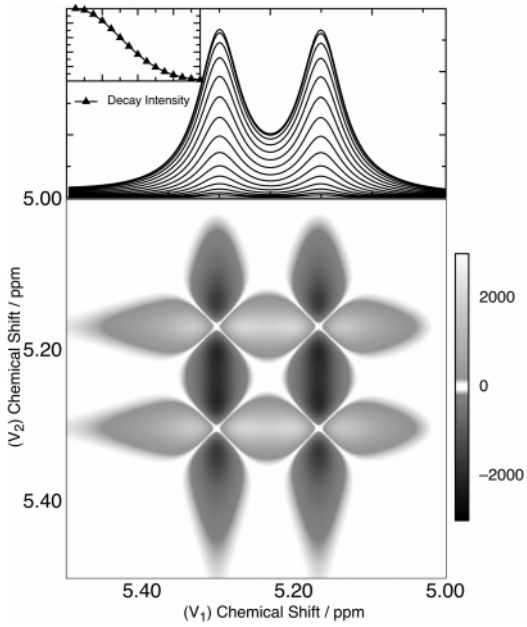

Figure 3. Simulation of the effect of peak-broadening on an asynchronous plot during a Gaussian decay of two Lorentzian resonances. Both resonance signals exhibit a "cross" shape centered about the resonance maximum; in this example, because the two Lorentzian resonances are overlapped slightly, the characteristic cross-correlations also overlap.

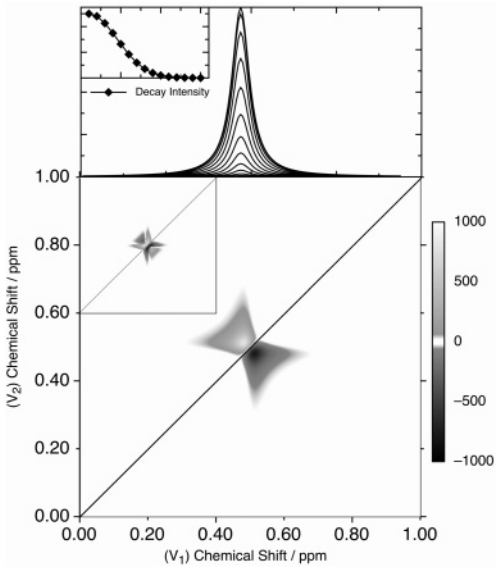

Figure 4. Simulation of frequency-shifting during the Gaussian decay of a single Lorentzian resonance. The asynchronous plot is very similar to two highly overlapped but independent resonances. The inset shows the characteristic "butterfly" pattern typically, which was obtained from the same data by correcting the decay by normalization of each resonance to a common maximum.

guished by the observation of the classically described "butterfly" pattern (e.g., inset in Figure 4). However, when the resonance is decaying in intensity, two of the six-lobes increase in correlation intensity toward the direction of shift while the remaining four decrease. This ultimately leads to a pattern that appears to be identical to that obtained for two highly overlapped independent resonances. An examination of the raw 1-dimensional data is always recommended to ensure that the "butterfly" pattern is not due to a systematic error in peak alignment.

This situation can be resolved quite easily by isolation of the resonance. The data can be integrated and normalized such that the maximum value for each perturbation at g is set equal

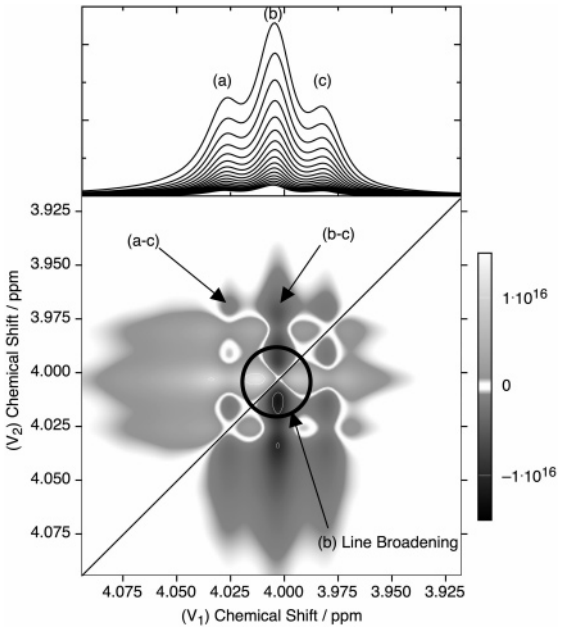

Figure 5. Asynchronous correlation map from DOSY data of pure linear polycaprolactone (PCL-1) in the OCH_2 region. The map shows the characteristic patterns of line broadening, the strongest signal of which is centered about the triplet maximum at $\delta = 4.004$ ppm.

to unity. The first derivative of the data can then be taken to regain the original form with the loss of only one data point. The data can then be re-evaluated: if the signal is due to two overlapped resonances, this "intermediate" correlation will return an overall null map, while a drifting signal will present a clear "butterfly". The effect of a loss of homogeneity should result in a systematic change in δ, and so the entire DOSY data can be shifted to common maxima. The situation described here is identical to an analysis of 1-dimensional spectra, where chemical shift corrections are made; for example, aligning the spectra to the internal standard TMS (0 ppm) or the proton resonance of $CHCl_3$ (7.26 ppm). This procedure can be automated in a postprocessing environment. Having a strong knowledge of the different DOSY artifacts and the ease at which these can be identified by application of GECO-DOSY greatly simplifies analysis of DOSY experiments.

By developing a good understanding of the common DOSY artifacts and how they can manifest themselves in GECO-DOSY, we have applied the technique to conventional acquired DOSY data, such as that presented in Figure 1. In the following sections, we demonstrate how GECO-DOSY can be used as a tool to evaluate polymer mixtures.

Pure Linear PCL. Figure 5 presents the GECO-DOSY analysis of linear PCL (PCL-1) for the OCH_2 methylene triplet of the ^{1}H NMR spectrum; the Lorentzian resonances responsible for this pattern are located at (a) $\delta = 4.026$, (b) $\delta = 4.004$, and (c) $\delta = 3.982$ ppm.

In addition to obvious correlation between the respective peaks, Figure 5 suggests that line broadening occurs during the DOSY experiment. This can be concluded from the intense "cross" shape, which is located about $\delta = 4.004$ ppm of the central resonance of the triplet (b). Line broadening, as opposed to narrowing, can be confirmed by examination of the correlation lobe signs, which are positive in the horizontal and negative in the vertical. The same pattern can be seen for the outer resonances of the triplet; their correlation intensity is somewhat less. Cross-correlations of the broadening resonances can be seen, especially about the central resonance (b). Because of the large intensity, A(δ), of this signal, each of the cross-correlations

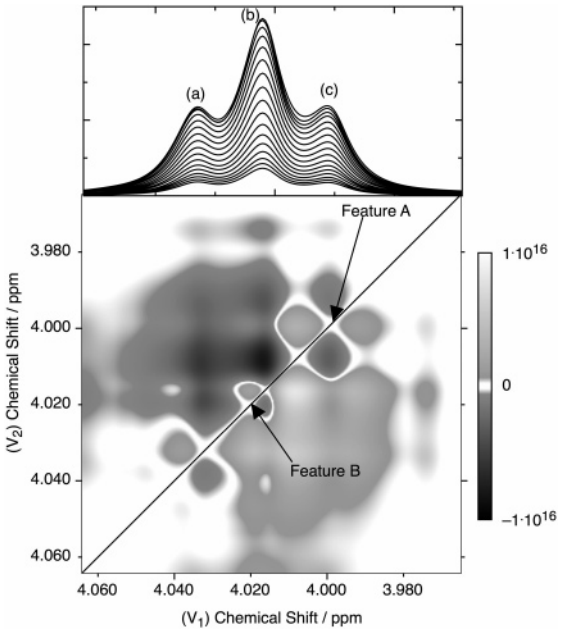

Figure 6. Asynchronous correlation map of DOSY data for PCL-2. The correlation map clearly shows the effects of line broadening, in addition to a contribution from additional species present in the mixture.

between this signal and the side peaks (a−b and b−c) is strong. However, cross-correlations between the two side peaks (a and c) is weaker, especially as these resonances overlap with the central resonance. The cross-correlations between (a) and (c) appear because, at any time during the experiment, the broadening of the two resonances results in two resonances that are out of phase with each other with respect to chemical shift. However, these cross-correlations do not mean that the resonances decay with different diffusion coefficients. On the contrary, the width of the lobes from the cross-correlations of the two outermost resonances show that they exhibit identical degrees of line broadening, as would be expected for resonances of equal initial intensity from the same chemical species. Therefore, this correlation map suggests that only a single chemical species is contributing to the signal intensity and this species has a single diffusion coefficient: purely linear PCL.

Cyclic/PLC Mixture. Figure 6 shows the GECO-DOSY analysis of the PCL-2 polymer sample that was produced via an enzymatic reaction. As can be seen in Figure 6, the GECO-DOSY analysis presents a different correlation plot than that observed for the linear sample in Figure 5. Immediately, this describes a chemically different system; a cursory analysis of this sample would suggest that the two-polymer systems exhibit significantly different dynamic behavior when subjected to the GECO-DOSY analysis. However, closer inspection reveals that the two samples both contain similar experimental artifacts. For example, both samples show a degree of line broadening (feature A in Figure 6) during the course of the DOSY experiment. The correlation map in Figure 6 appears to be more asymmetric about each of the Lorentzian resonances of the triplet compared to that of the linear system. This behavior cannot be explained by physical or instrumental effects. A possible explanation, brought about by noting the tight butterfly section (feature B in Figure 6), may be that the central Lorentzian resonance shifts in frequency during the course of the experiment, perhaps induced by a small temperature gradient. This hypothesis was tested by aligning the maximum value of the triplet resonance, as described previously. However, upon performing this correction, an identical GECO-DOSY correlation map was obtained, suggesting that a shifting frequency is not the explanation for these features. Hence, the presence of an additional component beneath the more prominent triplet of the linear PCL appears to be more probable.

It is the differences in *dynamic behavior* between PCL-1 and PCL-2 that create different correlation maps. These differences can be brought about by the introduction of other species of unique chemical shift and diffusion coefficients or by a deviation

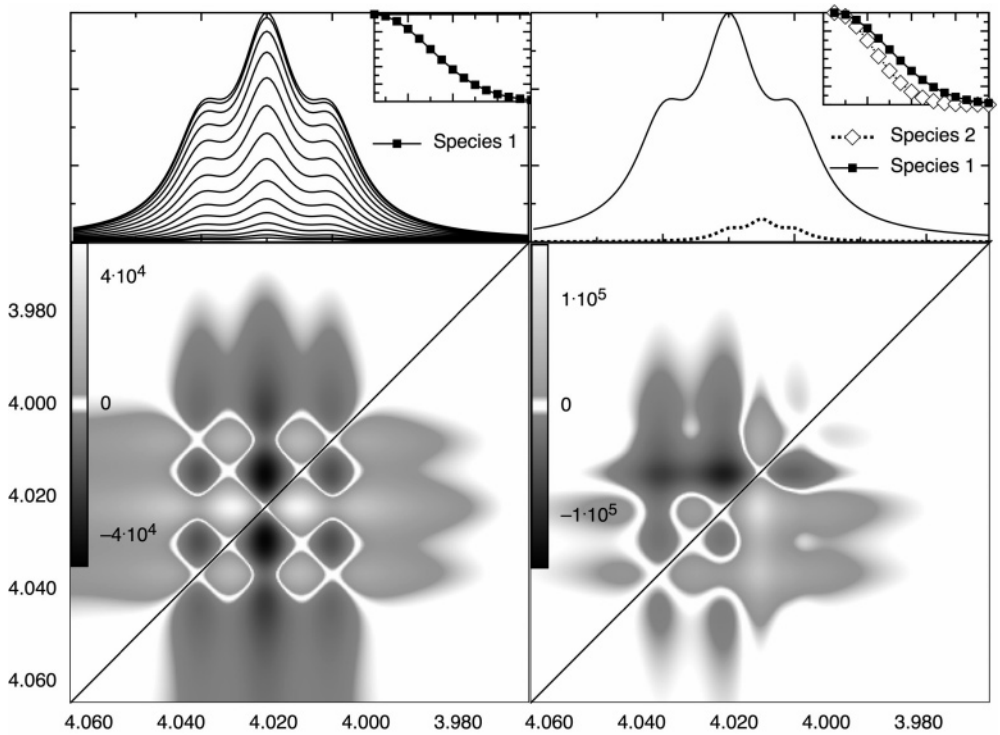

Figure 7. (A: left) Simulated correlation map of a Gaussian decayed triplet; the map shows the characteristic profile of line-broadening typical of our DOSY data. (B: right) The correlation map produced by the addition of another triplet resonance, species 2, offset and overlapping with species 1. The resonance signal intensities and Gaussian decay intensities are shown in the insets.

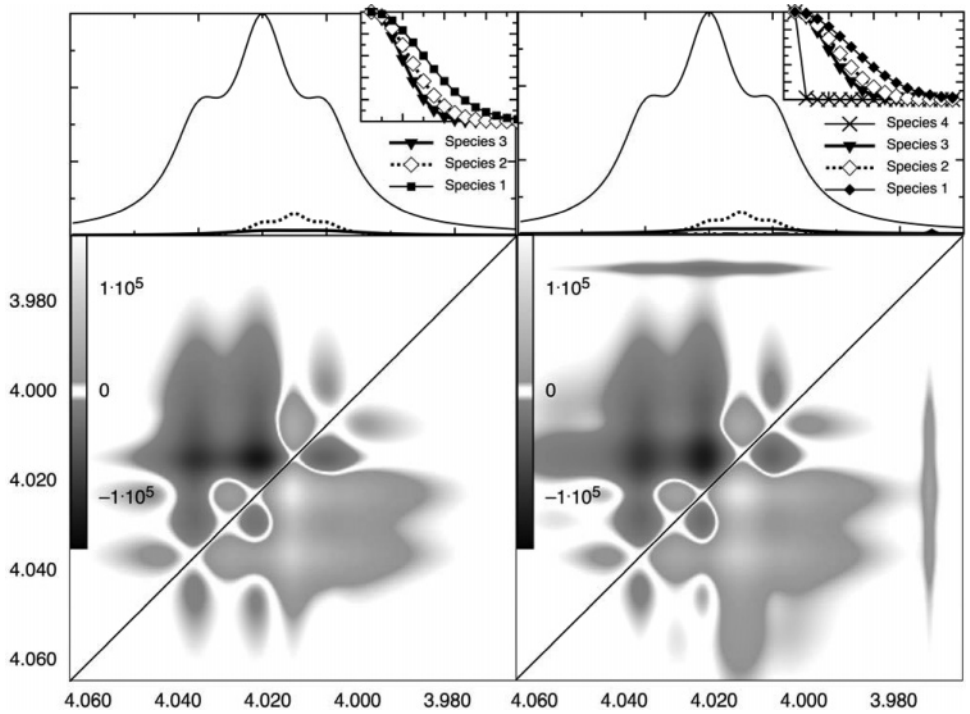

Figure 8. (A, left) The correlation map produced by the addition of an overlapped but weak doublet, species 3, to the data presented in Figure 7b. (B, right) The final simulation of PCl-2 formed by the addition of the rapidly, diffusing species 4 to the data presented in Figure 8a. The resonance signal intensities and Gaussian decay intensities are shown in the insets.

in the mechanism of line broadening. It is most probable that both of these contribute to the differences observed in this example. Small (cyclic) polymeric chains exhibit near-to-identical chemicals shifts to that of linear PCL. We have assigned the differences in the two correlation maps to the presence of these species. The presence of cyclics would manifest itself in two ways: First, a small chemical shift contrast in the Hertz range (of approximately several tens of Hz), would influence the dynamic behavior of the overwhelmingly large linear PCL resonances even though their A(δ) contributions are smaller. Second, the presence of these species, which have different diffusion coefficients, result in a different rate of line broadening, which contribute toward the dynamic behavior. The effect of introducing such a resonance in combination with the PCL line-broadened resonances is that species that diffuse quickly will produce resonances that dissipate rapidly from the DOSY experiment. The effect is that the contributions to the overall resonances change during the experiment, producing a unique dynamic behavior. Thus, the complicated profile evident in Figure 6 not only suggests the existence of other species in the sample, but also that these new species diffuse at a different rate from that of the major component. Such information was *impossible* to gain from analysis of the conventional DOSY data.

While such correlation maps clearly show the presence of additional species in the mixture, the ability to qualify such species would be a powerful additional benefit of GECO-DOSY. To this end, we have set about to simulate the correlation map observed in Figure 6 with these principles in mind and also to demonstrate these effects during the GECO-DOSY analysis. The simulations presented here are not intended to replicate all of the features of the GECO-DOSY map of Figure 6 but are intended to demonstrate the effects of perturbing the data by small underlying resonances from additional species and also to highlight the sensitivity toward these additional resonances.

First, a triplet of Lorentzian resonances at frequencies identical to those observed in PCL-1 (3.894, 4.0216, 4.007 ppm) were mathematically set up to decay in a Gaussian fashion, with a line broadening factor of 5%. The resulting correlation map (Figure 7a) possesses many of the features found in Figure 5, although more symmetrical. Figure 7a displays the entire simulated DOSY spectra, which decay to zero. The correlation map clearly describes three overlapped and broadening Lorentzian peaks. A second set of triplet resonances was added to the previous simulated dataset with frequencies $\delta = 4.0216$, 4.0145, and 4.007 ppm, the resulting correlation map of which is presented in Figure 7b.

The triplet resonances of species 2 act to skew the correlation map; this skew manifests itself in the form an antisymmetrical four-leafed clover pattern. The resonances of species 2 were set at 10-fold lower intensity than that of the simulated PCL-1 triplet resonances. It is interesting to note that, although two of the triplet resonances from species 2 have identical resonance frequencies to those found in the simulated PCL-1 signal, if these are removed from the simulation, the resulting GECO-DOSY map appears completely different, showing that the *dynamic* behavior of the overlapped resonances is unique. The addition of these extra resonances does not visually perturb the 1-dimensional data and it provides a good approximation for the correlation pattern obtained for PCL-2 in Figure 6 despite the cross-correlations lobes not being identical. Because *signal intensity* does not play a role in the overall *correlation intensity*, these differences cannot be due to larger amounts of species 2 resonances underneath the larger simulated PCL-1 signal. This disadvantage of GECO-DOSY means that, while the presence of extra species can be demonstrated, a quantitative analysis cannot be performed.

Further improvements in the simulation can be obtained by including another two species, diffusing at different rates, which act to further perturb this correlation map. Furthermore, this species must be diffusing at a faster rate in order to have a positive effect on the simulation. To this end, a doublet (4.0202 and 4.006 ppm) was added to produce Figure 8a. So as not to perturb the 1-dimensional data, species 3 has a signal intensity 20-fold weaker than the simulated PCL-1 signal. Although this

addition does not make a large difference to the overall simulation, it does add some of the features required, such as the enlargement of the correlations between 4.006 ppm and other resonances, and the weakening of the correlations between 4.0202 and 3.894 ppm. A final rapidly diffusing species at 3.975 ppm as a singlet was added to simulate the correlations observed in Figure 6 around this region. This is probably an impurity in the genuine PCL-2 sample.

The final simulation presented in Figure 8b shows a correlation map that exhibits many of the features found in the GECO-DOSY analysis of PCL-2 in Figure 6. Such a profile could only be simulated by the addition of an extra four uniquely diffusing species that lie beneath the main resonances of linear PCL-1. Although it is clear that the simulation is not an exact replica of the original dataset, it is important to highlight that these correlation maps are highly sensitive to slight deviations in broadening, diffusion, or peak shifting. The complex nature of NMR resonances and instrumentation means that simple Lorentzian peaks cannot simulate experimental data exactly. However, it is clear that three or more separate chemical species produce this pattern, a conclusion that cannot be made simply by traditional DOSY analysis. We believe that a combination of other postprocessing methodologies such as DECRA or MCR could provide a better basis for additional resonance frequencies, which would aid facilitation of a more accurate simulation.

The ability to perform GECO-DOSY analysis for the determination of chemical shift and diffusion information of these underlying peaks, without the need for complicated extraction methodologies, highlights the power of this analytical technique. GECO-DOSY provides unprecedented chemical shift and diffusional resolution, which we believe will greatly increase the value of this technique for future polymer analysis.

Conclusions

GECO-DOSY has provided a novel method for analysis of DOSY data for a complex polymer mixture. The technique provides useful information for the analysis of samples that have little chemical shift contrast between differently diffusing species. We have described the most commonly encountered experimental artifacts and demonstrated simple methods to eliminate or reduce these effects. We have shown that the differences in line broadening behavior of differently diffusing species may allow for an increased resolution to be obtained. Furthermore, the identification of three or more separate species in a PCL sample prepared by enzymatic methods has been possible when characterization and identification by traditional DOSY analysis was unsuccessful. We believe that GECO-DOSY will provide a rapid and simple method for extended analysis of DOSY data to provide information as to the speciation within polymer samples. This will provide the NMR spectroscopist with a complementary and inexpensive analysis tool for complex DOSY data, which may be an invaluable approach for use prior to further, more complex analytical techniques.

Acknowledgment. We thank the Research Councils UK: Basic Technology Programme (EP/C006763−J.R.H.), and the Dutch Polymer Institute (project 488−K.J.T.) for financial support. S.M.H. is a Royal Society Wolfson Research Merit Award Holder.

Supporting Information Available: Matlab scripts written in-house. This material is available free of charge via the Internet at http://pubs.acs.org.

References and Notes

(1) Nobes, G. A. R.; Kazlauskas, R. J.; Marchessault, R. H. *Macromolecules* **1996**, *29*, 4829−4833.
(2) Matsumura, S.; Tsukada, K.; Toshima, K. *Macromolecules* **1997**, *30*, 3122−3124.
(3) Matsumura, S.; Mabuchi, K.; Toshima, K. *Macromol. Rapid Commun.* **1997**, *18*, 477−482.
(4) Tasaki, H.; Toshima, K.; Matsumura, S. *Macromol. Biosci.* **2003**, *3*, 436−441.
(5) Bisht, K. S.; Svirkin, Y. Y.; Henderson, L. A.; Gross, R. A.; Kaplan, D. L.; Swift, G. *Macromolecules* **1997**, *30*, 7735−7742.
(6) Mei, Y.; Kumar, A.; Gross, R. A. *Macromolecules* **2002**, *35*, 5444−5448.
(7) Henderson, L. A.; Svirkin, Y. Y.; Gross, R. A.; Kaplan, D. L.; Swift, G. *Macromolecules* **1996**, *29*, 7759−7766.
(8) Duda, A.; Kowalski, A.; Penczek, S.; Uyama, H.; Kobayashi, S. *Macromolecules* **2002**, *35*, 4266−4270.
(9) Loeker, F. C.; Duxbury, C. J.; Kumar, R.; Gao, W.; Gross, R. A.; Howdle, S. M. *Macromolecules* **2004**, *37*, 2450−2453.
(10) Mei, Y.; Kumar, A.; Gross, R. *Macromolecules* **2003**, *36*, 5530−5536.
(11) Cordova, A.; Iversen, T.; Hult, K.; Martinelle, M. *Polymer* **1998**, *39*, 6519−6524.
(12) Callaghan, P. T. *Principles of Nuclear Magnetic Resonance Microscopy*; Clarendon Press: Oxford, 1991.
(13) Price, W. S. *Concepts Magn. Reson.* **1997**, *9*, 299−336.
(14) Johnson, C. S. *Prog. NMR Spectrosc.* **1999**, *34*, 203−256.
(15) Pelta, M. D.; Morris, G. A.; Stchedroff, M. J.; Hammond, S. J. *Magn. Reson. Chem.* **2002**, *40*, S147−S152.
(16) Loening, N. M.; Keeler, J.; Morris, G. A. *J. Magn. Reson.* **2001**, *153*, 103−112.
(17) Pelta, M. D.; Barjat, H.; Morris, G. A.; Davis, A. L.; Hammond, S. J. *Magn. Reson. Chem.* **1998**, *36*, 706−714.
(18) Jerschow, A.; Muller, N. *Macromolecules* **1998**, *31*, 6573−6578.
(19) Morris, K. F.; Johnson, C. S. *J. Am. Chem. Soc.* **1992**, *114*, 3139−3141.
(20) Ahn, S.; Kim, E. H.; Lee, C. *Bull. Korean Chem. Soc.* **2005**, *26*, 331−333.
(21) Chen, A.; Wu, D. H.; Johnson, C. S. *J. Am. Chem. Soc.* **1995**, *117*, 7965−7970.
(22) Kapur, G. S.; Findeisen, M.; Berger, S. *Fuel* **2000**, *79*, 1347−1351.
(23) Morris, K. F.; Johnson, C. S. *J. Am. Chem. Soc.* **1993**, *115*, 4291−4299.
(24) Antalek, B.; Windig, W. *J. Am. Chem. Soc.* **1996**, *118* (42), 10331−10332.
(25) Stilbs, P.; Paulsen, K.; Griffiths, P. C. *J. Phys. Chem.* **1996**, *100*, 8180−8189.
(26) Antalek, B. *Concepts in Magn. Reson.* **2002**, *14*, 225−258.
(27) Huo, R.; Geurts, C.; Brands, J.; Wehrens, R.; Buydens, L. M. C. *Magn. Reson. Chem.* **2006**, *44*, 110−117.
(28) Jayawickrama, D. A.; Larive, C. K.; McCord, E. F.; Roe, D. C. *Magn. Reson. Chem.* **1998**, *36*, 755−760.
(29) Van Gorkom, L. C. M.; Hancewicz, T. M. *J. Magn. Reson.* **1998**, *130*, 125−130.
(30) Eads, C. D.; Noda, I. *J. Am. Chem. Soc.* **2002**, *124*, 1111−1118.
(31) Sasic, S.; Jiang, J. H.; Sato, H.; Ozaki, Y. *Analyst* **2003**, *128*, 1097−1103.
(32) Czarnecki, M. A. *Chem. Phys. Lett.* **2003**, *368*, 115−120.
(33) Ozaki, Y.; Sasic, S.; Tanaka, T.; Noda, I. *Bull. Chem. Soc. Jpn.* **2001**, *74*, 1−17.
(34) Harrington, P. D.; Urbas, A.; Tandler, P. J. *Chemom. Intell. Lab. Syst.* **2000**, *50*, 149−174.
(35) Czarnecki, M. A.; Wu, P. Y.; Siesler, H. W. *Chem. Phys. Lett.* **1998**, *283*, 326−332.
(36) Noda, I. *Appl. Spectrosc.* **1993**, *47*, 1329−1336.
(37) Noda, I.; Dowrey, A. E.; Marcott, C.; Story, G. M.; Ozaki, Y. *Appl. Spectrosc.* **2000**, *54*, 236A−248A.
(38) Izawa, K.; Ogasawara, T.; Masuda, H.; Okabayashi, H.; O'Connor, C. J.; Noda, I. *Phys. Chem. Chem. Phys.* **2002**, *4*, 1053−1061.
(39) Hyde, J. R.; Walsh, B.; Poliakoff, M. *Angew. Chem.* **2005**, *44*, 7588−7591.
(40) Hyde, J. R.; Stephenson, P.; Poliakoff, M.; Bourne, R. *Anal. Chem.* **2004**, *76*, 6197−6206.
(41) Noda, I.; Ozaki, U. *Two Dimensional Spectroscopy*; John Wiley and Sons: New York, 2004; p 310.
(42) Noda, I. *Appl. Spectrosc.* **2000**, *54*, 994−999.
(43) Jerschow, A.; Muller, N. *J. Magn. Reson.* **1997**, *125*, 372−375.
(44) Huo, R.; Molengraff van de, R. A.; Pikkemaat, J. A.; Wehrens, R.; Buydens, L. M. C. *J. Magn. Reson.* **2005**, *172*, 342−358.
(45) We have opted to avoid using the more traditional ω used in the description of the generalized correlation function as to avoid confusion with the frequency of the NMR resonance at field strength, *B*.

MA061345Q